Dillon Stacey R. (Orcid ID: 0000-0001-8758-3795)

Title

Povetacicept, an Enhanced Dual APRIL/BAFF Antagonist that Modulates B Lymphocytes and Pathogenic Autoantibodies for the Treatment of Lupus and Other B Cell-Related Autoimmune Diseases

Authors

Lawrence S. Evans, BS†, Katherine E. Lewis, PhD†, Daniel DeMonte, PhD, Janhavi G. Bhandari, MSc, Logan B. Garrett, BSc, Joseph L. Kuijper, BSc, Daniel Ardourel, BSc, Martin F. Wolfson, BSc, Susan Debrot, BSc, Sherri Mudri, BSc, Kayla Kleist, MSc, Luana L. Griffin, BSc, LuAnne Hebb, AAS, MFA, Russell J. Sanderson, PhD, NingXin Wang, BSc, Michelle Seaberg, BSc, Allison G. Chunyk, MSc, Jing Yang, PhD, Youji Hong, BSc, Zahra Maria, PhD, David J. Messenheimer, PhD, Pamela M. Holland, PhD, Stanford L. Peng, MD, PhD, Mark W. Rixon, PhD, and Stacey R. Dillon, PhD

Lawrence S. Evans, BS†, Alpine Immune Sciences, Inc., Seattle, WA, USA
Katherine E. Lewis, PhD†, Alpine Immune Sciences, Inc., Seattle, WA, USA
Daniel DeMonte, PhD, Alpine Immune Sciences, Inc., Seattle, WA, USA
Janhavi G. Bhandari, MSc, Alpine Immune Sciences, Inc., Seattle, WA, USA
Logan B. Garrett, BSc, Alpine Immune Sciences, Inc., Seattle, WA, USA
Joseph L. Kuijper, BSc, Alpine Immune Sciences, Inc., Seattle, WA, USA
Daniel Ardourel, BSc, Alpine Immune Sciences, Inc., Seattle, WA, USA
Martin F. Wolfson, BSc, Alpine Immune Sciences, Inc., Seattle, WA, USA
Susan Debrot, BSc, Alpine Immune Sciences, Inc., Seattle, WA, USA
Sherri Mudri, BSc, Alpine Immune Sciences, Inc., Seattle, WA, USA
Kayla Kleist, MSc, Alpine Immune Sciences, Inc., Seattle, WA, USA
Luana L. Griffin, BSc, Alpine Immune Sciences, Inc., Seattle, WA, USA
LuAnne Hebb, AAS, MFA, Alpine Immune Sciences, Inc., Seattle, WA, USA
Russell J. Sanderson, PhD, Alpine Immune Sciences, Inc., Seattle, WA, USA
NingXin Wang, BSc, Alpine Immune Sciences, Inc., Seattle, WA, USA
Michelle Seaberg, BSc, Alpine Immune Sciences, Inc., Seattle, WA, USA
Allison G. Chunyk, Alpine Immune Sciences, Inc., Seattle, WA, USA
MSc, Jing Yang, PhD, Alpine Immune Sciences, Inc., Seattle, WA, USA
Youji Hong, BSc, Alpine Immune Sciences, Inc., Seattle, WA, USA

This article has been accepted for publication and undergone full peer review but has not been through the copyediting, typesetting, pagination and proofreading process which may lead to differences between this version and the Version of Record. Please cite this article as doi: 10.1002/art.42462

Zahra Maria, PhD, Alpine Immune Sciences, Inc., Seattle, WA, USA
David J. Messenheimer, PhD, Alpine Immune Sciences, Inc., Seattle, WA, USA
Pamela M. Holland, PhD, Alpine Immune Sciences, Inc., Seattle, WA, USA
Stanford L. Peng, MD, PhD, Alpine Immune Sciences, Inc., Seattle, WA, USA
Mark W. Rixon, PhD, Alpine Immune Sciences, Inc., Seattle, WA, USA
Stacey R. Dillon, PhD, Alpine Immune Sciences, Inc., Seattle, WA, USA

[†]These authors contributed equally to this work

Address Correspondence to Stacey R. Dillon Alpine Immune Sciences, Inc., 188 East Blaine St., Suite 200, Seattle, WA 98102. E-mail: Stacey.Dillon@alpineimmunesciences.com

Running head: Povetacicept, an Engineered TACI-Fc with Enhanced Dual APRIL/BAFF Antagonism

Financial Interests

This study was supported by Alpine Immune Sciences, Inc.
L.S.E., K.E.L, D.D., J.G.B., L.B.G., J.L.K., D.A., M.F.W., S.D., S.M., K.K., L.L.G., L.H., R.J.S., N.W., M.S., A.G.C., J.Y., Y.H., Z.M., D.J.M., P.M.H., S.L.P., M.W.R., and S.R.D. are current or former employees and shareholders of Alpine Immune Sciences, Inc.

Abstract

Objective. Dysregulated APRIL/BAFF signaling is implicated in the pathogenesis of multiple autoimmune diseases, including SLE and LN. A high affinity APRIL/BAFF antagonist was developed to overcome the clinical limitations of existing B cell inhibitors.

Methods. A variant of TACI-Fc generated by directed evolution showed enhanced binding for both APRIL and BAFF and was designated povetacicept (ALPN-303). Povetacicept was compared to WT TACI-Fc and related molecules in vitro and in vivo.

Results. Povetacicept inhibited APRIL and BAFF more effectively than all evaluated forms of WT TACI-Fc, and selective APRIL and BAFF inhibitors, in cell-based reporter assays and primary human B cell assays, mediating potent suppression of B cell proliferation, differentiation, and immunoglobulin secretion. In mouse immunization models, povetacicept significantly reduced serum Ig titers and antibody-secreting cells more effectively than anti-CD20 mAb, WT TACI-Fc, or APRIL and BAFF inhibitors. In the NZB/W lupus nephritis model, povetacicept significantly enhanced survival and suppressed proteinuria, anti-double stranded DNA antibody titers, blood urea nitrogen, glomerulonephritis, and renal Ig deposition. In the bm12 lupus model, povetacicept significantly reduced splenic plasmablasts, T_{FH}, and germinal center B cells. In non-human primates, povetacicept was well-tolerated and exhibited high serum exposure and significantly decreased serum IgM, IgA, and IgG levels after a single dose.

Conclusion. Enhanced APRIL and BAFF inhibition by povetacicept leads to greater inhibition of B cell populations critical for autoantibody production versus WT TACI-Fc and CD20-, APRIL-, or BAFF-selective inhibitors. Potent, dual inhibition by povetacicept has the potential to significantly improve clinical outcomes in autoantibody-related autoimmune diseases.

Introduction

B cells have long been implicated in autoimmune diseases such as systemic lupus erythematosus (SLE), owing to their ability to present antigen to autoreactive T cells, secrete inflammatory cytokines (1), and differentiate into antibody-secreting cells (ASC), i.e., plasmablasts and plasma cells (PC), that are responsible for the production of pathogenic autoantibodies (2). Therefore, depletion or inhibition of B cells and ASC represents a compelling approach for many rheumatic and other autoimmune disorders.

Key modulators of B cell development, differentiation, and survival include the tumor necrosis factor (TNF) family cytokines, B cell activating factor (BAFF; TNFSF13B) and a proliferation-inducing ligand (APRIL; TNFSF13), which are expressed primarily by myeloid cells and signal through multiple receptors. BAFF binds with varying affinity to B cell-expressed BAFF-R (TNFRSF13C), transmembrane activator and calcium-modulating cyclophilin ligand interactor (TACI; TNFRSF13B), and B cell maturation antigen (BCMA; TNFRSF17), while APRIL binds TACI and BCMA (3) and heparin sulfate proteoglycans (HSPG). BAFF can exist in three functional forms: membrane-bound, soluble trimer, and soluble BAFF 60-mer (4), with the soluble trimer formed via proteolytic cleavage of membrane BAFF (3). APRIL and BAFF can also form functionally active heterotrimers; all forms of these cytokines have been shown to be elevated in various antibody-related diseases, including SLE (5, 6).

Despite structural similarities and engagement of common signaling pathways, APRIL and BAFF play non-redundant roles in B cell regulation, due in part to differential receptor expression at partially overlapping stages of B cell development. While BAFF plays key roles earlier in B cell development when BAFF-R is expressed, APRIL assumes a key role in the function of differentiated ASC that express TACI, BCMA, and HSPG (e.g., syndecan-1/CD138). Among several B cell targeting strategies, blockade of BAFF or APRIL has shown clinical promise. Belimumab is an anti-BAFF antibody approved for the treatment of SLE (7) and SLE-related lupus nephritis (LN) (8), but clinical remission as measured by Lupus Low Disease Activity State (LLDAS) or Complete Renal Response (CRR) is achieved in only a minority of patients, (12-4% or 30%, respectively) (9, 10). Thus, there remains a need for more active agents. Other BAFF/APRIL-targeting antibodies include ianalumab, a blocking and cell-depleting anti-BAFF-R antibody (11), and the anti-APRIL antibodies BION-1301 (12) and sibeprenlimab (VIS649) (13). These antibodies have demonstrated promising pharmacodynamic

activity in Phase 1 clinical trials (14, 15), but are limited by only inhibiting either BAFF or APRIL (3, 16-21). BAFF-Trap, a WT TACI and WT BAFF-R hybrid Fc-fusion protein (22) also shares limitations by inhibiting only BAFF.

Atacicept (3) and telitacicept (23) are soluble WT TACI extracellular domain (ECD) Fc-fusion proteins that strongly inhibit BAFF and weakly inhibit APRIL signaling. Atacicept and telitacicept have both demonstrated clinical activity in SLE (23-25). However, atacicept formally failed to meet its primary endpoint in pivotal trials (24) and appears to no longer be in active development for SLE (26). In contrast, telitacicept has been conditionally approved in China for the treatment of SLE based on a phase 2b study, and recently reported positive confirmatory phase 3 results; however, most subjects appear to have still flared within the first 6 months of treatment (Wu D., et al. American College of Rheumatology Convergence 2022, abstract #L07). These findings provide clinical validation of the BAFF/APRIL pathway for SLE, but also suggest that further improvement upon the drug designs of atacicept and telitacicept, perhaps by improving APRIL inhibition in particular, may afford a unique opportunity to achieve more effective yet safe therapeutic options.

Herein we describe the engineering of a modified TACI domain to generate povetacicept (ALPN-303), a potent inhibitor of both APRIL and BAFF. We show that modifications in the TACI domain of povetacicept translate to enhanced target binding affinity and inhibitory activity compared to WT TACI-Fc in vitro, and greater immunoglobulin suppression over comparators in mouse immunization and SLE disease models. We postulate that improved dual APRIL and BAFF inhibition will provide more effective and durable relief from severe autoimmune diseases in which B cells and antibody responses play a role.

Materials and Methods

Proteins and Cell Lines

Recombinant APRIL and BAFF were purchased from Tonbo Biosciences and BioLegend, respectively. BAFF 60-mer was from AdipoGen. Belimumab was either generated at AIS (and designated ‘anti-BAFF mAb’), using the variable region sequence available from PDB ID 5Y9K and an attenuated effector function activity IgG1 constant region, or was directly sourced (Benlysta®) through Myonex. WT TACI-Fc based on the atacicept sequence from SEQ ID NO:

54 from US Patent 8,815,238 B2 was generated at AIS and designated 'WT TACI 30-110-Fc.' WT TACI-Fc based on the telitacicept sequence included with the WHO INN submission found in WHO Drug Information, Vol. 32, No. 4, 2018, was generated at AIS and designated 'WT TACI 13-118-Fc.' Additionally, telitacicept (Tai'ai®) was sourced through Clinigen. Anti-APRIL mAb VIS649 (sibeprenlimab) was generated at AIS based on the sequence included with the WHO INN submission found in WHO Drug Information, Vol. 34, No. 4, 2020 for sibeprenlimab. Anti-APRIL mAb BION-1301 was generated at AIS based on SEQ ID NO: 50 and 52 from US Patent Appl. US 2020/0079859 A1. Mouse (m) BAFF-R-Fc fusion protein and anti-mAPRIL mAb 4540 (13) were generated at AIS using a mouse Fc (mouse IgG1 D265A) with reduced effector function. Single chain heterotrimeric APRIL and BAFF (comprising both the 2A:1B and 1A:2B forms) and a single chain BAFF homotrimer were generated based on published sequences (27). Jurkat cells containing an NF-κB luciferase reporter NF-κB were obtained from BPS Bioscience. A summary of all comparator reagents used in these studies is provided in Supplementary Table 1.

Yeast Surface Display Mutagenesis Libraries and Recombinant Protein Expression

Yeast surface display libraries containing randomly mutated TACI variants (designated variable TNFR domains, or "vTD") were generated as described (28). Recombinant WT TACI and TACI vTD-Fc-fusion proteins were generated via transient expression in Expi293F™ cells (ThermoFisher Scientific) per the manufacturer's instructions. Protein was purified from conditioned media harvests by capture and elution from Protein A and formulated in 25 mM Tris, 161 mM arginine, pH 7.5. Material was tested for endotoxin levels (LAL endotoxin kit, Charles River Laboratories) and all proteins contained <1 EU/mg.

TACI/Jurkat/NF-κB reporter assay

Jurkat/NF-κB cells were transduced with lentivirus to yield stable surface expression of human or mouse TACI (TACI/Jurkat/NF-κB), both of which demonstrate species cross-reactivity with APRIL and BAFF ligands. Recombinant human APRIL or BAFF (1-10 nM) were incubated with fixed or titrated (200 nM-2.5 pM) TACI domain-containing molecules or comparators. Ligands and inhibitors or Fc controls were incubated for 20 min shaking (150 rpm) at room temperature (RT) prior to the addition of 1.5 x 10^5 TACI/Jurkat/NF-κB cells/well within a white 96-well flat bottom plate. Plates were incubated 5 hours at 37 °C, after which luciferase substrate solution

(Bio-Glo™ Luciferase Assay System, Promega) was added while shaking (150 rpm) for 10 minutes. Relative luminescence units (RLU) were determined using a Cytation 3 (BioTek Instruments) or SpectraMax iD3 (Molecular Devices) imaging reader.

Binding Affinity Measurement by Surface Plasmon Resonance

Affinity determination was conducted on a Biacore 3000 optical biosensor equipped with a CM5 sensor chip (GE) prepared with goat anti-human IgG capture antibody (Jackson ImmunoResearch). Povetacicept was captured to a level of 30 response units (RU) for the APRIL kinetic assays and 50 RU for the BAFF kinetic assays. Telitacicept was captured to a level of 135 RU for the APRIL kinetic assays and 145 RU for the BAFF kinetic assays. BAFF and APRIL concentrations (100 nM-0.137 nM) were prepared in running buffer (HBS-EP buffer system: 10 mM HEPES pH 7.4, 150 mM NaCl, 3 mM EDTA, and 0.05% Surfactant P20). Association phases were monitored for 240 s at a flow rate of 30 µL/min, and the dissociation phases for 400 s were captured at the same flow rate. A long dissociation experiment was run for the BAFF interactions using the 33.3 nM concentration for 1800 s at a flow rate of 30 µL/min. Data were aligned, double referenced, and fit using Scrubber v2.0® software (BioLogic Software Pty Ltd).

Human B Cell Differentiation Assay

CD19+ B cells were isolated from human peripheral blood mononuclear cells (PBMC) (n=8 donors) using negative selection kits (StemCell Technologies), activated with 2 nM recombinant human (rh) CD40L for 3 days, washed, and incubated another 4 days with 50 ng/mL rhIL-21 + 10 nM BAFF + 10 nM APRIL. Supernatants were collected for serum Ig analysis and assayed using an immunoglobulin MILLIPLEX® kit (EMD Millipore, # HGAMMAG-301K) with magnetic beads and antibodies specific for detecting soluble IgM, IgA, IgG1, IgG2, IgG3, and IgG4. Results were analyzed in GraphPad Prism®. For APRIL+BAFF cultures, the percent inhibition of Ig secretion was determined using the following formula: ([Median APRIL+BAFF Ig value - Experimental Ig value]/Median APRIL+BAFF Ig value) x 100. Cells were harvested, stained with LiveDead blue (Invitrogen), anti-human IgM, -IgD, -CD27, -CD38, and -CD319 (BioLegend) and analyzed by flow cytometric analysis for B cell subset and plasma cell survival and differentiation. The gating strategy and exemplary contour plots for naïve B, class switched memory B, and plasma cells for each treatment condition are provided in Supplementary Figure

4, and Supplementary Table 4 is a summary of the concentrations (ng/mL) of secreted Ig in the supernatants for each treatment condition.

In vivo Models

Animal Husbandry Ethical Approval

Mouse studies were approved by the Institutional Animal Care and Use Committee (IACUC) overseeing the vivarium where studies were conducted (Alpine Immune Sciences or Hooke Laboratories, Lawrence MA), and followed the guidelines set forth in the 8th Edition of the Guide for the Care and Use of Laboratory Animals (National Research Council, 2011). The cynomolgus monkey study was conducted with approval from the Altasciences (Everett, WA) Preclinical IACUC.

Mouse Keyhole Limpet Hemocyanin (KLH) Immunization Model

WT male C57BL/6NJ mice (10 weeks old; Jackson Laboratory) were randomly assigned into 5 groups (n=5). All mice except the naïve control group were immunized with 250 μg KLH (Cat 374825-25MG; EMD Millipore) in Dulbecco's PBS (Gibco-ThermoFisher Scientific) via IP injection on Day 0 and 12. Mice received either Fc control, povetacicept, WT TACI 30-110-Fc, or WT TACI 13-118-Fc by IP injection on Days 4 and 11, molar matched to 15 mg/kg povetacicept. Mice were sacrificed on Day 20, and blood and spleens were collected for serum anti-KLH Ig analysis and splenocyte immunophenotyping.

Mouse Sheep Red Blood Cell (SRBC) Immunization Model

WT female BALB/cJ mice (8 weeks old; Jackson Laboratory) were randomly assigned into groups of 4 to 8 each. All but the naïve control group were immunized with 25 μL of citrated sheep blood (Colorado Serum Co.) via IP injection on Day 0. Test articles were delivered via IP injection on Days 1 and 6 and dosed as indicated for each study in the figure legends. Mouse anti-CD20 mAb (clone SA271G2) was from BioLegend. Mice in each study were sacrificed on Day 15, and blood, spleen, and bone marrow were collected for serum anti-SRBC analysis and splenocyte and bone marrow immunophenotyping.

NZB/W Spontaneous Lupus Model

Female NZB/W F_1 mice (22 weeks old; Jackson Laboratory), randomized to 2 groups (n=15 each) based on their levels of serum anti-dsDNA antibodies and proteinuria, received either 17

mg/kg povetacicept or a molar-matched Fc control IP, 2x/week for 20 weeks, until termination at Week 43. Body weights were taken, and proteinuria measured weekly using urine dip sticks (Chemstrip™ 2 GP; Roche). Proteinuria was scored 0 to 4, (0 = no detectable protein, 1 = <30 mg/dL, 2 = 30 to 100 mg/dL, 3 = 100 to 500 mg/dL, 4 = >500 mg/dL). Anti-dsDNA antibodies were measured throughout the study and at termination; serum levels of blood urea nitrogen (BUN) were measured in terminal samples (IDEXX Laboratories, Inc.). At 43 weeks of age (or earlier if mice were moribund), the left kidneys were collected in 10% neutral buffered formalin for hematoxylin and eosin (H&E) or periodic acid-Schiff staining, and the right kidneys were embedded in Optimal Cutting Temperature (OCT) compound (Tissue-Tek®, Sakura Finetek) and evaluated for IgG by IHC. Stained sections were scored for glomerular IgG deposition (29). Submandibular glands were collected, weighed, fixed in 10% neutral buffered formalin (NBF) for 48 hours, and embedded in paraffin blocks for histopathological analysis of sialadenitis. Data from flow cytometry analyses to evaluate immune cell subsets at termination (Week 43) were not reliable enough to include herein due to 1) the lack of representative Fc control-treated mice surviving early termination due to disease severity, and 2) the relatively low cell viability observed following overnight shipment of the spleens and lymph nodes. Of the samples that could be analyzed, the patterns of B cell reductions expected based on prior mouse model studies (e.g., reduced frequency of total B220+, transitional-2, marginal zone, and follicular B) were observed in the povetacicept-treated group.

bm12 Inducible Model of Lupus

Spleens and inguinal lymph nodes from 28 female I-A^{bm12}B6(C)-*H2*-Ab1^{bm12}/KhEgJ (‘bm12’) mice (8 to 11 weeks old; Jackson Laboratory) were injected IP as single cell suspensions to 26 WT female C57BL/6NJ recipient mice (8 to 9 weeks old; Jackson Laboratory) on Day 0 (30) to mice that had been randomly assigned to 2 groups. On Day 5, test articles were delivered via IP injection and dosed as indicated in figure legends, continuing 2x/week until 6 days before termination on Day 95. Six female age matched C57BL/6NJ mice were naïve, untreated controls. At termination, spleens were collected for flow cytometry and the left kidney embedded in OCT compound as described above until evaluated for IgG staining by immunohistochemistry (IHC).

Flow Cytometry Analyses for Mouse Studies

Spleens and bone marrow cells were processed into single cell suspensions, RBC were lysed with 1X RBC Lysis Buffer (BioLegend) per manufacturer's instructions, and cells were counted. Live cells (1×10^6) were then stained with antibodies listed in Supplementary Table 2 for flow cytometry analysis of immune cell subsets following live-dead staining (LIVE/DEAD Fixable Aqua or Blue Dead Cell Stain Kit, Life Technologies Corp; 1:1000 dilution in DPBS) and pre-incubation with Mouse BD Fc Block (Becton-Dickinson). Stained cells were collected on an LSRII (Becton-Dickinson) or CytoFLEX LX (Beckman Coulter) flow cytometer. Flow cytometry gating examples are provided in Supplementary Figures 6-7. Data were analyzed using FlowJo software (FlowJo LLC) and graphed using GraphPad Prism® software.

Non-Human Primate Pharmacokinetics (PK)/Pharmacodynamics (PD) Study

Povetacicept and WT TACI 13-118-Fc (9 mg/kg each) were evaluated after a single 30-minute IV infusion on Day 0 to two female cynomolgus monkeys per group. Control animals received vehicle (25 mM Tris, 161 mM arginine, pH 7.5) under the same conditions. Blood was collected at various timepoints (predose and at 0.083, 2, 6, 24, 72, 144, 312, 480, 624, 816, and 984 hours post-end of infusion) through Day 26 to characterize test article serum concentrations, while blood sampling continued through Day 42 to assess serum concentrations of IgM, IgA, and IgG. Noncompartmental analysis was conducted, and PK parameters were estimated, using Phoenix WinNonlin software (Pharsight Corp/Certara). Serum IgM, IgA, and IgG was measured at Altasciences as part of a standard serum chemistry panel of analytes.

Statistical Analysis

Statistically significant differences between groups were determined using one-way analysis of variance (ANOVA) and uncorrected Fisher's least significant difference multiple comparison test (KLH model; SRBC IgM, IgG1, IgG2a data in Figure 4A, plasma cell and plasmablast data in Figure 4D-G; SRBC IgG1, IgG2a, IgG2b, and T_{FH} data in Supplementary Figure 8), Kruskal-Wallis test and uncorrected Dunn's test (human B cell assay; SRBC IgG2b data in Figure 4A, and GC and T_{FH} data in Figure 4B-C; bm12 model; SRBC IgM, plasma cell, and GC data in Supplementary Figure 8), unpaired two-tailed Mann-Whitney test (single time point data in the NZB/W model), two-way repeated measures ANOVA (data over time in the NZB/W model), or the Mantel-Cox log-rank test (survival analysis in the NZB/W model). Normality testing was

performed to select the appropriate statistical method. The naïve groups in the KLH, SRBC, and bm12 models were not included in the statistical analyses. No animals were excluded from analysis in any in vivo model. GraphPad PRISM® (version 9.0.2) was used for statistical analyses and p values < 0.05 were considered statistically significant for all tests.

Results

Engineering and Characterization of an Optimized APRIL and BAFF Inhibitor

The ECD of TACI consists of two TNFR cysteine-rich domains (CRDs) and a stalk region (Supplementary Figure 1A). APRIL and BAFF binding sites on TACI are located within CRD2 (31). Therefore, the single TACI CRD2 domain was selected for further optimization using a directed engineering approach to enhance binding of TACI CRD2 to APRIL and BAFF. Libraries containing mutagenized TACI CRD2 were generated via error-prone PCR and selected for enhanced APRIL and BAFF binding through yeast surface display (28) (Supplementary Figure 2A, 2B**)**. Selected TACI variant TNFR domain (TACI vTD) hits were fused to a human IgG1 Fc lacking effector function (32), expressed in mammalian cells and evaluated in the TACI/Jurkat/NF-κB reporter assay (Supplementary Figure 2C). The highest-ranking candidate, TACI vTD H88-Fc, was designated ALPN-303 (povetacicept). The inhibitory activity of povetacicept in the TACI/Jurkat/NF-κB assay was approximately 19-fold and 14-fold greater than WT TACI 13-118-Fc for neutralization of APRIL or BAFF, respectively (Figure 1A, Supplementary Table 3). Povetacicept bears three amino acid substitutions within TACI CRD2: K77E, F78Y, and Y102D, all three of which appear necessary for optimal activity, because all single- and double-substitution revertant-containing versions exhibited decreased inhibitory activity relative to povetacicept (data not shown). By surface plasmon resonance, the affinity of povetacicept for BAFF (59.3 pM) was approximately 8-fold better than that of telitacicept (491 pM); its affinity for APRIL was approximately 1 pM, while telitacicept's affinity for APRIL was not able to be determined due to multiple on- and off-rates (Figure 1B-C).

Povetacicept Inhibits APRIL and BAFF More Potently than Comparator Molecules In Vitro

The ability of povetacicept to inhibit APRIL and BAFF activity alone or in combination was measured in the TACI/Jurkat/NF-κB reporter assay relative to comparator APRIL and/or BAFF inhibitors (summarized in Supplementary Table 3) including telitacicept, the anti-BAFF antibody

belimumab, and an anti-APRIL mAb derived from the published sequence for BION-1301 (12). Povetacicept effectively neutralized APRIL 5.7-fold better than the anti-APRIL mAb, and neutralized BAFF 3.4-fold better than belimumab (Figure 2A, Supplementary Table 3). Povetacicept was also the most potent inhibitor of the combination of APRIL and BAFF, with a >50-fold lower IC_{50} value relative to telitacicept, and a 3.5-fold better IC_{50} value relative to the combination of anti-APRIL mAb plus belimumab (Figure 2A, Supplementary Table 3).

APRIL and BAFF can form heterotrimeric proteins at 2:1 ratios (5, 6). Additionally, soluble BAFF exists in a high molecular weight complex designated as BAFF 60-mer (4). Inhibition of APRIL and BAFF trimers/heterotrimers as well as BAFF 60-mer is likely required for full inhibition of these pathways in autoimmune settings where multiple forms of these ligands can be present and/or elevated (4). Povetacicept was tested for its ability to inhibit BAFF 60-mer- and APRIL/BAFF heterotrimer-induced signaling in the TACI/Jurkat/NF-κB assay. Povetacicept inhibited BAFF 60-mer significantly better (p<0.0001) than the full-length WT TACI-Fc proteins tested (Supplementary Figure 3A, 3E). In addition, single chain heterotrimers of APRIL and BAFF were generated, consisting of BAFF-APRIL-APRIL (BAA) and ABB formats to represent both possible forms (27). A single chain BAFF homotrimer was included as a control. Povetacicept demonstrated greater inhibition against the BAFF homotrimer and BAFF/APRIL heterotrimers as compared to telitacicept (Supplementary Figure 3B-E**)**. An anti-APRIL antibody produced from the published sequence for VIS649 (sibeprenlimab) only inhibited the BAA heterotrimer, while belimumab inhibited the ABB heterotrimer (in contrast to previously published results (27)) and the BAFF homotrimer. Collectively, these findings indicate that directed engineering of a single TACI CRD2 domain is sufficient to generate significantly enhanced affinity for APRIL and increased BAFF affinity, resulting in inhibitory activity superior to clinically relevant therapeutics, including monoclonal antibodies.

Povetacicept Inhibits Class-Switched (CSw) Memory B Cell and Plasma Cell Survival and Ig Secretion More Potently than Telitacicept, anti-APRIL, or anti-BAFF in Primary Human B Cell Assays

We next evaluated the ability of povetacicept to affect primary human B cell proliferation, differentiation, and Ig secretion in vitro. Purified human pan B cells were first stimulated for 3 days with recombinant CD40L and then plated for 4 days in the presence of exogenous BAFF,

APRIL, and test articles. As compared to telitacicept, anti-APRIL mAb, or anti-BAFF mAb, povetacicept more potently inhibited expansion of total B cells and various key B cell subsets, including class-switched (CSw) memory B cells and plasma cells (Figure 2B, Supplementary Figure 4). This potent inhibition of B cell expansion and survival by povetacicept also correlated with significant reductions in Igs secreted into the culture media (Figure 2C, 2D, Supplementary Table 4). These findings are consistent with the ability of povetacicept to inhibit the differentiation of naïve B cells to plasma cells with activity superior to anti-BAFF or anti-APRIL mAbs, confirming that co-inhibition of both APRIL and BAFF results in greater suppression of Ig secretion compared to blockade of either cytokine alone. In addition, povetacicept demonstrated superior activity as compared to telitacicept in this assay, consistent with its improved affinity for APRIL and BAFF.

Povetacicept Inhibits APRIL and BAFF More Potently than Comparator Molecules in Mouse Immunization Models

To determine if the enhanced APRIL and BAFF blockade observed with povetacicept in vitro translated into enhanced activity in vivo, povetacicept was evaluated in a mouse KLH immunization model. Notably, povetacicept and comparators inhibit mouse and human APRIL and BAFF with comparable relative IC_{50} values (Supplementary Table 3). Mice were challenged with KLH as a model antigen and then treated with povetacicept or WT TACI-Fc comparators to assess their immunomodulatory activity. KLH immunization increased spleen size and cellularity as shown by the significant increase in splenocyte numbers in the Fc control-treated group compared to the naïve group (Figure 3A, Supplementary Figure 5A). Mice treated with povetacicept on Days 4 and 11 following KLH immunization on Day 0 had significantly reduced total spleen cellularity at the end of the study (Day 20) compared to mice treated with Fc control, WT TACI 30-110-Fc, or WT TACI 13-118-Fc (Figure 3A, Supplementary Figure 5). Except for the least mature transitional type-1 (T1) B cells, all splenic B cell subsets evaluated (gated as defined in Supplementary Figures 6-7), including transitional type 2 (T2), follicular, marginal zone (MZ), germinal center (GC), and plasma cells were significantly reduced following povetacicept treatment, exceeding the activity of WT TACI-Fc (Figure 3A-B, Supplementary Figure 5A).

There was no significant effect on the numbers of splenic T cells with povetacicept, WT TACI 30-110-Fc, or WT TACI 13-118-Fc treatment (Supplementary Figure 5B). In contrast, the total

numbers of CD4+ T follicular helper (T_{FH}) cells per spleen were significantly lower in each of the treatment groups compared to Fc control, with povetacicept treatment mediating the greatest reductions (Figure 3C). Povetacicept also significantly reduced the formation of anti-KLH IgM and IgG1 antibodies at Day 20, reflecting its impact on a primary humoral immune response (Figure 3D). The reductions in the anti-KLH Ig concentrations observed with povetacicept were significantly greater than those mediated by WT TACI-Fc.

Povetacicept was also evaluated for its impact on the antibody response to another T cell-dependent antigen in a primary SRBC immunization model. Following SRBC immunization, mice were dosed twice with Fc control, povetacicept, telitacicept, an anti-mAPRIL mAb, mBAFF-R-Fc, or a combination of anti-mAPRIL and mBAFF-R-Fc. Mice were sacrificed on Day 15, and spleens and bone marrow were processed for immunophenotyping by flow cytometry. Serum titers of anti-SRBC IgM and IgG were also measured. Povetacicept demonstrated significantly enhanced immunosuppressive activity over all of the comparators, including the combination of anti-mAPRIL + mBAFF-R-Fc, for most of the endpoints, including reduced anti-SRBC Ig responses (Figure 4A), decreased numbers of splenic GC B cells (Figure 4B), T_{FH} cells (Figure 4C), PC (Figure 4D), and plasmablasts (Figure 4E), as well as reductions in the percent of LL-PC (Figure 4F) and total PC in the bone marrow (Figure 4G). Similar SRBC immunization studies were conducted to compare the activity of povetacicept to telitacicept and a depleting mouse anti-CD20 antibody. Povetacicept again demonstrated enhanced immunosuppressive activity over WT TACI CRD2-Fc, telitacicept, and anti-CD20 as determined by endpoints similar to those listed above (Supplementary Figure 8). Collectively, the results from these immunization studies demonstrate that the optimized dual inhibition of APRIL and BAFF by povetacicept provides deeper and more sustained ASC and B cell suppression as compared to anti-CD20, telitacicept, inhibitors of either APRIL or BAFF alone, or a combination of APRIL and BAFF inhibitors, leading to greater suppression of T cell-dependent antibody responses.

Povetacicept Suppresses Disease in Spontaneous and Inducible Models of SLE

Povetacicept was next evaluated in the NZB/W spontaneous mouse model of lupus. In this model, NZB mice are bred to NZW mice and by 6 months of age, mice develop severe lupus-like features similar to those of human lupus patients. The model is characterized by the presence of serum antinuclear autoantibodies (including anti-dsDNA), mild vasculitis, and the development

of immune complex-mediated glomerulonephritis (33). In this study, 22-week-old NZB/W mice were randomized based on serum anti-dsDNA Ab titers and proteinuria and treated twice weekly with povetacicept or an Fc control for up to 20 weeks. As compared to treatment with Fc control, povetacicept treatment provided protection from disease, including reduced proteinuria and development of anti-dsDNA IgG autoantibodies (Figure 5A-B). Moreover, povetacicept treatment significantly improved survival, suppressed BUN, reduced histopathological scores for sialadenitis, and reduced glomerulonephritis and deposition of renal IgG (Figure 5C-H). Povetacicept was also evaluated in the bm12 inducible model, in which lupus-like disease is induced by injecting C57BL/6NJ mice with MHC-mismatched bm12 splenocytes. Glomerular IgG immune deposits are evident by ~4 weeks following splenocyte transfer. Mice were treated with povetacicept or an Fc control twice weekly from Days 5 through 88. Glomerular IgG deposits were significantly elevated in this model at the end of the study (Day 95), and povetacicept significantly reduced these deposits as compared to Fc control-treated mice (Figure 5I-J). Furthermore, povetacicept treatment resulted in significantly lower numbers of splenic plasma cells, GC B cells, and T_{FH} cells (Figure 5K-M) as compared to the Fc control, similar to what was observed in the KLH and SRBC immunization models.

Povetacicept Suppresses Serum Ig in Cynomolgus Monkeys

A PK/PD study in cynomolgus monkeys was conducted to evaluate povetacicept relative to WT TACI 13-118-Fc, both administered at a single 9 mg/kg IV dose. Dose-normalized serum concentrations of the test articles and serum IgM, IgA, and IgG levels are shown in Figure 6A; published atacicept PK data (34) are overlaid for comparison, based on a 1 mg/kg IV administration to cynomolgus monkeys. Both test articles were well-tolerated, and serum concentrations of povetacicept and WT TACI 13-118-Fc were measurable to Day 26 postdose. Time to maximum concentration (T_{max}) was observed at the first collection time point following the end of infusion (0.083 hours post end of infusion) for both test articles. Exposure was similar between the two test articles based on the maximum serum concentration (C_{max}). However, based on the area under the curve from time 0 to the last time t (AUC_{0-t}), exposure was 3 to 4 times higher after povetacicept dosing compared to WT TACI 13-118-Fc. The dose-normalized C_{max} (µg/mL per mg/kg) values were 27, 25, and 23, and the dose-normalized AUC (µg*hr/mL per

mg/kg) values were 1167, 397, and 215 for povetacicept, WT TACI 13-118-Fc, and atacicept, respectively.

The levels of serum IgM, IgA, and IgG in animals receiving povetacicept decreased an average of approximately 60%, 50%, and 30% at their nadir on Day 27, respectively, as compared to pre-dose levels (Figure 6B). In comparison, the serum Ig decreases from baseline in animals treated with WT TACI 13-118-Fc versus pre-dose levels were much less dramatic (~20% decreases in IgM, no apparent impact on IgA, and ~15% reduction in IgG).

Discussion

SLE and other autoantibody-related rheumatic diseases remain indications of high unmet need. In SLE, treatment options have been hindered by complex pathogenesis and heterogeneity of disease, suggesting that multiple pathways or aspects of B cell development and differentiation may require simultaneous inhibition to enable durable responses. While B cell-depleting agents such as rituximab/ocrelizumab/obinutuzumab (anti-CD20), and obexelimab (anti-CD19) have exhibited favorable clinical impacts in certain autoimmune disease settings, this has not translated to SLE, where rituximab failed to demonstrate benefit in SLE and LN trials (35, 36). One possible limitation of these therapeutics is that CD20 and CD19 are not expressed on all ASC or LL-PC, and only earlier stage B cells (including pro/pre, immature, mature, and memory B cells) are depleted, sparing most pathogenic plasmablasts and PC (37).

Targeting or co-targeting BAFF and/or APRIL has garnered increasing interest as an alternative to ADCC-mediated B cell depletion. Preclinical studies have demonstrated that starving B cells of these two critical B cell survival and differentiation factors can significantly reduce all B cell subsets beyond the immature T1 stage of development, including LL-PC, without affecting CD19+CD20+ pro/pre-B cell precursors (38). Inhibition of ASC can dramatically impact pathogenic antibody production and thereby potentially reduce disease activity. Although early efforts to target the BAFF/APRIL pathway focused on agents like belimumab that neutralize only BAFF, a preponderance of preclinical data suggest that inhibition of both APRIL and BAFF is required to impact survival of more differentiated, pathogenic $TACI^{+}$/$BCMA^{+}$ ASC (3).

APRIL plays a particularly important role in IgA class switching, production, and glycosylation, as first indicated by studies of APRIL knockout mice (39). In addition, elevated plasma APRIL levels in IgA nephropathy (IgAN) patients are associated with more severe clinical manifestations such as high proteinuria and Gd (galactose deficient) IgA1 levels (40), which are important causal factors and contribute to disease pathogenesis. Indeed, early trials of BION-1301 and sibeprenlimab suggest that APRIL-only inhibition can mediate significant decreases in Ig (particularly IgA) in healthy subjects, and BION-1301 impacts proteinuria in IgAN patients in an ongoing trial (41). However, targeting APRIL alone has its own limitations and would not be expected to impact less mature BAFF-dependent B cells that can also contribute to disease pathogenesis (37). BAFF neutralization leads to downregulation of B cell function, decreases in

autoantibody production, and inhibition of tertiary lymphoid structure formation in the kidney (3).

Belimumab was the first approved therapy for SLE and LN after a 50-year drought (37), underscoring the need for new therapies. Another development in SLE therapy was the recent approval of anifrolumab an anti-type I interferon receptor antibody (42, 43). Anifrolumab targets a distinct pathophysiology of SLE from B cell modulators, by targeting myeloid dendritic cells rather than B cells, although type I interferons are known to indirectly promote B cell differentiation and loss of tolerance. IFN-regulated gene expression is significantly increased in SLE; however, interferon gene signature expression has not been predictive of response, underscoring the pleiotropic effects of the IFN system (42). In contrast, the presence of high serum levels of BAFF and APRIL in patients with SLE is well established and has been described in numerous studies (3). High serum BAFF levels also correlate with elevated autoantibody levels, particularly anti-dsDNA Abs (3).

Until now, co-targeting BAFF and APRIL has been attempted only with development of the WT TACI-Fc molecules atacicept and telitacicept, though the affinity of WT TACI-Fc for APRIL is arguably suboptimal, well below that achieved by anti-APRIL mAbs, which range in affinity from K_D= 0.95 to 400 pM, depending on the method used (Figure 1; (12, 13). Thus, while these molecules arguably neutralize BAFF sufficiently, their inefficient blockade of APRIL activity leaves clear room for improvement. Reports of affinity-enhanced soluble BCMA fusion proteins as an alternate approach to co-target APRIL and BAFF were recently described, and may be in pre-clinical development, though their structure and mutational burden have not yet been disclosed (Morales S et al. American College of Rheumatology Convergence 2022, Abstract #1629) (44). Povetacicept addresses the limitations of WT TACI-Fc by dramatically improving the affinity of TACI for both APRIL and BAFF (Figure 1), leading to functional neutralizing activity both in vitro (Figure 2) and in vivo (Figures 3-5). Moreover, a single dose of povetacicept led to notably enhanced suppression of serum immunoglobulins relative to WT TACI 13-118-Fc in a non-human primate study (Figure 6). The higher serum exposures and more potent immunomodulatory activities observed with povetacicept may enable improved efficacy, lower clinical doses, and/or longer dosing intervals compared to other TACI-Fc molecules. For example, whereas telitacicept is generally dosed 1x/week, povetacicept is

anticipated to be administered once at least every 4 weeks, based on exposure and pharmacodynamic observations.

A theoretical safety concern regarding povetacicept's highly potent inhibition of BAFF and APRIL is infection, especially considering prior reports of increased infection risk with agents such as rituximab (45-47) or atacicept (48). Such findings may however have been confounded by the use of prior concomitant immunosuppressive medications and/or inadequate safety monitoring, such as of circulating Ig levels (49). Indeed, the most recently studied drug in this class in SLE, telitacicept, appears to be well tolerated so far without a clear imbalance in infectious events, such as upper respiratory tract infections or herpes zoster (25, 50). As such, careful safety monitoring of subjects treated with povetacicept will be warranted during its clinical trials, hopefully affording eventual determination of a potently effective yet safe dose regimen.

The potent immunosuppressive activity of povetacicept in vitro and in spontaneous and inducible models of SLE (Figure 2, Figure 5) suggest it could be a superior therapeutic candidate in B cell-related autoimmune diseases where both APRIL and BAFF are dysregulated, and in settings where pathogenic autoantibodies contribute to disease progression. Whereas rituximab is used in standard practice in off-label settings, TACI is expressed on a broader range of B cell and plasma cell subsets compared to CD20, particularly antibody-producing plasmablasts and plasma cells. Since these ASC are considered the primary source of pathogenic autoantibodies in SLE, combined inhibition of BAFF and APRIL with povetacicept therefore has potential for greater efficacy. In addition to SLE, antibody associated glomerular diseases including LN and IgAN, as well as autoantibody-associated dermatoses, hematologic diseases, and neurological diseases might be better controlled with povetacicept treatment.

The limitations of these studies relate to the inherent caveats associated with animal models of human disease. Mouse lupus models cannot fully reproduce human clinical pathology; however, the NZB/W lupus model is well regarded as a tool for evaluating therapeutic candidates, since it develops spontaneously and with several, though not all, characteristics similar to those observed in lupus patients (18, 19, 51) In our study, dosing began when the NZB/W mice were 22 weeks old, when mice typically start displaying signs of lupus. However, markers of disease activity

such as anti-dsDNA antibodies and proteinuria were still relatively low at that stage and therefore the dosing regimen we evaluated cannot be considered fully therapeutic and instead better represents an 'early intervention' regimen. In the mouse KLH and SRBC immunization models, povetacicept dosing resulted in significantly lower numbers of plasma cells, though because dosing occurred early in the models, the observed PC reduction may be due to a blockade in plasma cell generation rather than effects on the survival of existing plasma cells, as this was not directly evaluated in our experiments. Future studies are planned to evaluate the impact of povetacicept on recall responses and on memory B cells that upon re-activation can develop into antibody-producing, short-lived PC. Additionally, we have defined long-lived PC (LL-PC) in our mouse studies using a previously described immunophenotype (i.e., viable $TACI^{high}$, $CD138^{high}$, B220-, CD19- cells) (52), though we did not formally confirm the functionality of cells bearing this phenotype in our experiments. Future studies could include, for example, adoptive transfer experiments with tagged/labeled B cells as a more definitive way to define and track long-lived PC following immunization. Finally, it should also be noted that the evaluation of povetacicept in the primary human B cell assay may not fully reflect the effects of treatment in humans. Nevertheless, the correlation between the observed activity of povetacicept in the mouse models and in the human primary B cell assay support the potential clinical translatability of our results.

Povetacicept was designed to overcome the shortcomings of BAFF or APRIL specific inhibitors and improve the affinity of WT TACI towards APRIL. By targeting both BAFF and APRIL, povetacicept has the potential to achieve superior efficacy in heterogeneous autoimmune disease settings such as SLE. Clinical trials of povetacicept in B cell- and/or autoantibody-related autoimmune diseases are strongly warranted and will enable the first clinical evaluation of potent co-inhibition of both APRIL and BAFF. A Phase 1 trial of povetacicept in adult healthy volunteers (NCT05034484) has been initiated to enable such studies (Dillon S. et al. American College of Rheumatology Convergence 2022, Abstract #0987).

Data availability

The data that support the findings of this study are included in the manuscript and in the Supplementary information.

Acknowledgements

The authors thank our colleagues, past and present, at Alpine Immune Sciences and particularly Steve Levin, Sean MacNeil, Wayne Gombotz, Josiah Brown, Mike Salema, Leah Zielinski, Andrea Peng, Chelsea Gudgeon, Erika Rickel, Kristine Swiderek, Mark Maurer, Jason Stubrich, and Jan Hillson for their contributions to the development of povetacicept. We gratefully acknowledge Olympic Protein Sciences for performing the SPR analyses, Hooke Laboratories for conducting the NZB/W study, Altasciences for conducting the cynomolgus monkey PK/PD study, and Kelly Byrnes-Blake for analyzing the PK data. We also gratefully acknowledge the medical writing/editing support of Julie Crider, Nan Luo, and Kristen Howery.

Author contributions:

D.D., J.G.B., L.B.G., J.L.K., D.A., M.F.W., and L.H. conducted directed evolution experiments and protein production.

L.S.E., K.E.L, D.D, M.F.W., A.G.C., and S.R.D. conceived and designed the studies.

L.S.E., S.D., S.M., K.K., N.W., and M.S. performed the in vitro experiments and analyzed the data.

K.E.L., S.M., K.K., L.L.G., J.Y., Y.H, Z.M., D.J.M. and S.R.D. designed and/or performed the animal studies.

R.J.S., P.M.H, S.L.P., M.W.R. and S.R.D. supervised studies.

P.M.H., M.W.R., K.E.L., and S.R.D. prepared the manuscript with input from all co-authors.

References

1. Lund FE. Cytokine-producing B lymphocytes-key regulators of immunity. Curr Opin Immunol 2008;20:332-8.
2. Banchereau R, Hong S, Cantarel B, et al. Personalized immunomonitoring uncovers molecular networks that stratify lupus patients. Cell 2016;165:551-65.
3. Samy E, Wax S, Huard B, et al. Targeting BAFF and APRIL in systemic lupus erythematosus and other antibody-associated diseases. Int Rev Immunol 2017;36:3-19.
4. Eslami M, Schneider P. Function, occurrence and inhibition of different forms of BAFF. Curr Opin Immunol 2021;71:75-80.
5. Roschke V, Sosnovtseva S, Ward CD, et al. BLyS and APRIL form biologically active heterotrimers that are expressed in patients with systemic immune-based rheumatic diseases. J Immunol 2002;169:4314-21.
6. Dillon SR, Harder B, Lewis KB, et al. B-lymphocyte stimulator/a proliferation-inducing ligand heterotrimers are elevated in the sera of patients with autoimmune disease and are neutralized by atacicept and B-cell maturation antigen-immunoglobulin. Arthritis Res Ther 2010;12:R48.
7. Hahn BH. Belimumab for systemic lupus erythematosus. N Engl J Med 2013;368:1528-35.
8. Asif S, Bargman J, Auguste B. A review of the AURORA and BLISS trials: will it revolutionize the treatment of lupus nephritis? Curr Opin Nephrol Hypertens 2022;31:278-82.
9. Oon S, Huq M, Golder V, et al. Lupus Low Disease Activity State (LLDAS) discriminates responders in the BLISS-52 and BLISS-76 phase III trials of belimumab in systemic lupus erythematosus. Ann Rheum Dis 2019;78:629-33.
10. Furie R, Rovin BH, Houssiau F, et al. Two-year, randomized, controlled trial of belimumab in lupus nephritis. N Engl J Med 2020;383:1117-28.
11. McWilliams EM, Lucas CR, Chen T, et al. Anti-BAFF-R antibody VAY-736 demonstrates promising preclinical activity in CLL and enhances effectiveness of ibrutinib. Blood Adv 2019;3:447-60.
12. Dulos J. Bion-1301: a novel fully blocking APRIL antibody for the treatment of multiple myeloma. America Society of Hematology; 2016 December 2 2016; San Diego, CA: Blood; 2016. p. 2112.
13. Myette JR, Kano T, Suzuki H, et al. A proliferation inducing ligand (APRIL) targeted antibody is a safe and effective treatment of murine IgA nephropathy. Kidney Int 2019;96:104-16.
14. Barratt J. Pharmacodynamic and clinical responses to BION-1301 in patients with IgA nephropathy: initial results of a Ph1/2 trial. American Society of Nephrology; 2021; On Demand, Virtual Only; 2021.
15. Mathur M, Barratt J, Suzuki Y, et al. Safety, tolerability, pharmacokinetics, and pharmacodynamics of VIS649 (sibeprenlimab), an APRIL-neutralizing IgG(2) monoclonal antibody, in healthy volunteers. Kidney Int Rep 2022;7:993-1003.

16. Ramanujam M, Wang X, Huang W, et al. Similarities and differences between selective and nonselective BAFF blockade in murine SLE. J Clin Invest 2006;116:724-34.
17. Benson MJ, Dillon SR, Castigli E, et al. Cutting edge: the dependence of plasma cells and independence of memory B cells on BAFF and APRIL. J Immunol 2008;180:3655-9.
18. Haselmayer P, Vigolo M, Nys J, et al. A mouse model of systemic lupus erythematosus responds better to soluble TACI than to soluble BAFFR, correlating with depletion of plasma cells. Eur J Immunol 2017;47:1075-85.
19. Huard B, Tran NL, Benkhoucha M, et al. Selective APRIL blockade delays systemic lupus erythematosus in mouse. PLoS One 2012;7:e31837.
20. Liu Z, Davidson A. BAFF inhibition: a new class of drugs for the treatment of autoimmunity. Exp Cell Res 2011;317:1270-7.
21. Stohl W, Yu N, Chalmers S, et al. Development of murine systemic lupus erythematosus in the absence of BAFF. Arthritis Rheumatol 2020;72:292-302.
22. Zhou B, Zhang H, Su X, et al. Therapeutic effects of a novel BAFF blocker on arthritis. Signal Transduct Target Ther 2019;4:19.
23. Shi F, Xue R, Zhou X, et al. Telitacicept as a BLyS/APRIL dual inhibitor for autoimmune disease. Immunopharmacol Immunotoxicol 2021;43:666-73.
24. Merrill JT, Wallace DJ, Wax S, et al. Efficacy and safety of atacicept in patients with systemic lupus erythematosus: results of a twenty-four-week, multicenter, randomized, double-blind, placebo-controlled, parallel-arm, phase IIb study. Arthritis Rheumatol 2018;70:266-76.
25. Dhillon S. Telitacicept: first approval. Drugs 2021;81.
26. Vera. Vera therapeutics provides business update and reports second quarter 2022 financial results. 2022.
27. Schuepbach-Mallepell S, Das D, Willen L, et al. Stoichiometry of heteromeric BAFF and APRIL cytokines dictates their receptor binding and signaling properties. J Biol Chem 2015;290:16330-42.
28. Levin SD, Evans LS, Bort S, et al. Novel immunomodulatory proteins generated via directed evolution of variant IgSF domains. Front Immunol 2020;10:3086.
29. Kelkka T, Kienhöfer D, Hoffmann M, et al. Reactive oxygen species deficiency induces autoimmunity with type 1 interferon signature. Antioxid Redox Signal 2014;21:2231-45.
30. Klarquist J, Janssen EM. The bm12 inducible model of systemic lupus erythematosus (SLE) in C57BL/6 mice. J Vis Exp 2015:e53319.
31. Hymowitz SG, Patel DR, Wallweber HJ, et al. Structures of APRIL-receptor complexes: like BCMA, TACI employs only a single cysteine-rich domain for high affinity ligand binding. J Biol Chem 2005;280:7218-27.

32. Hezareh M, Hessell AJ, Jensen RC, et al. Effector function activities of a panel of mutants of a broadly neutralizing antibody against human immunodeficiency virus type 1. J Virol 2001;75:12161-8.
33. Dixon FJ, Andrews BS, Eisenberg RA, et al. Etiology and pathogenesis of a spontaneous lupus-like syndrome in mice. Arthritis Rheum 1978;21:S64-7.
34. Carbonatto M, Yu P, Bertolino M, et al. Nonclinical safety, pharmacokinetics, and pharmacodynamics of atacicept. Toxicol Sci 2008;105:200-10.
35. Merrill JT, Neuwelt CM, Wallace DJ, et al. Efficacy and safety of rituximab in moderately-to-severely active systemic lupus erythematosus: the randomized, double-blind, phase II/III systemic lupus erythematosus evaluation of rituximab trial. Arthritis Rheum 2010;62:222-33.
36. Rovin BH, Furie R, Latinis K, et al. Efficacy and safety of rituximab in patients with active proliferative lupus nephritis: the Lupus Nephritis Assessment with Rituximab study. Arthritis Rheum 2012;64:1215-26.
37. Lee DSW, Rojas OL, Gommerman JL. B cell depletion therapies in autoimmune disease: advances and mechanistic insights. Nat Rev Drug Discov 2021;20:179-99.
38. Gross JA, Dillon SR, Mudri S, et al. TACI-Ig neutralizes molecules critical for B cell development and autoimmune disease. impaired B cell maturation in mice lacking BLyS. Immunity 2001;15:289-302.
39. Castigli E, Scott S, Dedeoglu F, et al. Impaired IgA class switching in APRIL-deficient mice. Proc Natl Acad Sci U S A 2004;101:3903-8.
40. Zhai YL, Zhu L, Shi SF, et al. Increased APRIL expression induces IgA1 aberrant glycosylation in IgA nephropathy. Medicine (Baltimore) 2016;95:e3099.
41. Barratt J, Kooienga L, Hour B, et al. Updated interim results of a phase 1/2 study to investigate the safety, tolerability, PK, PD, and clinical activity of BION-1301 in patients with IgA nephropathy. Nephrol Dial Trans 2022;37:gfac067.11.
42. Morand EF, Furie R, Tanaka Y, et al. Trial of anifrolumab in active systemic lupus erythematosus. N Engl J Med 2020;382:211-21.
43. Deeks ED. Anifrolumab: first approval. Drugs 2021;81:1795-802.
44. Miao YR, Thakkar K, Cenik C, et al. Developing high-affinity decoy receptors to treat multiple myeloma and diffuse large B cell lymphoma. J Exp Med 2022;219:e20220214.
45. Tudesq JJ, Cartron G, Rivière S, et al. Clinical and microbiological characteristics of the infections in patients treated with rituximab for autoimmune and/or malignant hematological disorders. Autoimmun Rev 2018;17:115-24.
46. Marco H, Smith RM, Jones RB, et al. The effect of rituximab therapy on immunoglobulin levels in patients with multisystem autoimmune disease. BMC Musculoskelet Disord 2014;15:178.

47. Varley CD, Winthrop KL. Long-term safety of rituximab (risks of viral and opportunistic infections). Curr Rheumatol Rep 2021;23:74.
48. Kaegi C, Steiner UC, Wuest B, et al. Systematic review of safety and efficacy of atacicept in treating immune-mediated disorders. Front Immunol 2020;11:433.
49. Ginzler EM, Wax S, Rajeswaran A, et al. Atacicept in combination with MMF and corticosteroids in lupus nephritis: results of a prematurely terminated trial. Arthritis Res Ther 2012;14:R33.
50. Telitacicept for Injection [Package insert]. Shandong, China: Rongchang Biopharmaceutical (Yantai) Co., Ltd., 9 March 2021.
51. Cornaby C, Elshikha AS, Teng X, et al. Efficacy of the combination of metformin and CTLA4Ig in the (NZB x NZW)F1 mouse model of lupus nephritis. Immunohorizons 2020;4:319-31.
52. Pracht K, Meinzinger J, Daum P, et al. A new staining protocol for detection of murine antibody-secreting plasma cell subsets by flow cytometry. Eur J Immunol 2017;47:1389-92.

Figure Legends

Figure 1. Assessment of APRIL and BAFF inhibitory activity and binding by various TACI Fc-fusion proteins and affinity optimized TACI variant povetacicept. **A.** APRIL and BAFF inhibition by the indicated TACI variants and povetacicept evaluated in the TACI/Jurkat/NF-κB reporter assay. Increased inhibitory activity is indicated by reduced luciferase production. **B**. Affinity measurements of povetacicept and telitacicept binding to recombinant human APRIL and BAFF as determined by SPR. **C.** SPR sensorgrams with povetacicept and telitacicept at medium density shown in black lines and results from non-linear least squares regression analysis of the data shown in orange lines. Telitacicept was sourced through Clinigen. Analyte concentrations were prepared in running buffer, ranging from 33.3 nM to 0.137 nM for APRIL and 33.3 nM to 0.412 nM for BAFF in 3-fold serial dilution steps.

Figure 2. Povetacicept inhibits APRIL and BAFF more potently than comparator molecules. **A**. APRIL, BAFF, or APRIL plus BAFF inhibition by povetacicept and the indicated comparator molecules was evaluated in the TACI/Jurkat/NF-κB reporter assay. **B**. CD19+ B cells were activated with rhCD40L and re-cultured with exogenous APRIL, BAFF, and povetacicept or the indicated comparator molecules. Cells were stained and analyzed by flow cytometry to identify class switched memory B cells (IgD, IgM, CD27+) or plasma cells (IgM, IgD, CD38+, CD319+). **C.** and **D.** CD19+ B cells were activated as in (B). After 7 days, supernatants were collected and IgM, IgA (**C**), IgG1, IgG2, IgG3, and IgG4 (**D**) secretion was quantitated by multiplex analysis. Telitacicept was sourced through Clinigen and belimumab obtained from Myonex. Statistically significant differences between group median values were determined using the Kruskal-Wallis test and uncorrected Dunn's test; p values < 0.05 were considered statistically significant.

Figure 3. Povetacicept reduces splenic immune cell subsets and inhibits T cell-dependent antibody formation more potently than telitacicept in KLH-immunized mice. C57BL/6NJ mice were challenged with KLH on Days 0 and 12 and dosed IP with povetacicept, Fc control, or WT TACI-Fc comparators (molar matched to 10 mg/kg povetacicept) on Days 4 and 11. **A.** Splenic B cell subsets (total number of cells/spleen) from KLH-challenged or naïve mice at Day 20, enumerated by flow cytometry. Individual data plots for B cell subsets and T cells are in Supplementary Fig. 4. **B**. Splenic plasma cells from 'B', with individual mice plotted. **C**. Total

number of T_{FH} cells/spleen from KLH-challenged or naïve mice at Day 20, enumerated by flow cytometry, with individual mice plotted. **D.** Day 20 serum samples were analyzed for KLH-specific IgM or IgG1 with results for individual mice shown. Data are presented as the mean ± SD.

Figure 4. Povetacicept demonstrates enhanced immunosuppressive activity over telitacicept and BAFF- or APRIL-only inhibitors in a mouse SRBC immunization model. **A.** Following SRBC immunization on Day 0, female BALB/cJ mice were dosed twice (IP), on Days 1 and 6, with 10 mg/kg povetacicept, Fc control, telitacicept, anti-mAPRIL mAb, mBAFF-R-Fc, or a combination of 10 mg/kg each anti-mAPRIL mAb + mBAFF-R-Fc. **A.** Anti-SRBC Ig concentrations in serum were measured on Day 15. The total number of germinal center (GC) B cells/spleen (**B**), CD4+ T_{FH} cells/spleen **(C)**, plasma cells (PC)/spleen **(D)**, and plasmablasts (PB)/spleen **(E)** were enumerated by flow cytometry, with values for individual mice plotted. The percentage of viable long-lived plasma cells (LL-PC, defined as $TACI^{high}CD138^{high}$B220- CD19-), **(F)** and total plasma cells (PC; $TACI^{high}CD138^{high}$ cells) **(G)** in the bone marrow were also determined by flow cytometry, with data for individual mice plotted. Data are presented as median ± interquartile range **(B-C)** or mean ± SD **(D-G).**

Figure 5. Povetacicept suppresses disease in SLE models. **A-H.** NZB/W F_1 mice received 17 mg/kg povetacicept or molar-matched Fc control IP every 3-4 days from 22-42 weeks of life for 40 total doses. **A-B**. Mean proteinuria scores (+SEM), anti-dsDNA IgG levels (+SEM) and survival curves over time. **D**. Serum BUN levels (mean±SD) at termination (Week 43). **E.** Median (±interquartile range) submandibular gland histopathological scores. **F-H**. Kidney histology (mean±SD) and IgG deposit score from left kidney at termination. Score is a sum of total glomerular, tubular, and interstitial lesions. **G.** Renal IgG deposit score (mean±SD) evaluated by IHC, from right kidney at termination. **H**. Representative IHC (10X) of renal IgG deposits from Fc control or povetacicept-treated mouse. **I-M.** C57BL/6NJ mice were injected IP with bm12 splenocytes on Day 0, dosed 2x/week (IP) Day 5 to Day 88 (6 days prior to termination), with 10 mg/kg povetacicept or molar-matched Fc control. Age-matched naïve mice served as controls. **I**. Renal IgG deposit score (median+interquartile range) evaluated by IHC for individual mice from left kidney at termination. **J**. Representative IHC (20X) of renal IgG deposits from Fc control, povetacicept (DAPI overlay in bottom right), or naïve mouse. **K-M**.

Total plasma cells, GC B cells, or CD4+ T_{FH} cells/spleen (median+ interquartile range), enumerated by flow cytometry, with individual mice plotted.

Figure 6. Povetacicept exhibits increased exposure and enhanced Ig suppression vs. WT TACI 13-118-Fc in non-human primates. **A.** Female cynomolgus monkeys (2 per treatment group) were administered a single 30-minute IV infusion on Day 0 of vehicle (0 mg/kg) or 9 mg/kg povetacicept or WT TACI 13-118-Fc. Serum was collected at various timepoints (pre-dose and at 0.083, 2, 6, 24, 72, 144, 312, 480, 624, 816, and 984 hour post-end of infusion), and samples were analyzed for test article concentrations using an ELISA method; dose normalized concentration curves are shown. Atacicept PK data from a 1 mg/kg IV administration were obtained from a publication (34). **B.** Levels of serum IgM, IgA, and IgG (mean + range) in each treatment group were measured by ELISA at various timepoints and plotted as a percentage of baseline serum concentrations obtained from serum collected on Day -8.

Supplementary Figure 1. TACI and BCMA full length and soluble TACI Fc-fusion protein domain structures and sequence alignment of the WT TACI and BCMA CRDs. **A.** Schematic diagrams indicating the protein domains of WT full length TACI and BCMA aligned with soluble TACI Fc-fusion proteins. The relative location of the mutations in povetacicept are indicated by ▼. CRD, cys rich domain; S, stalk; TMD, transmembrane domain; ICD, intracellular domain; Fc, IgG domain; black boxes represent Gly-Ser linker sequences. **B.** Aligned sequences of the TACI and BCMA CRD regions indicating locations of disulfide bonds. Shared identical residues are indicated by the grey shading. Sequences are numbered according to their UniProt entries; TACI-UniProtKB - O14836 (TR13B_HUMAN) and BCMA UniProtKB - Q02223 (TNR17_HUMAN). Mutations in TACI vTD H88 are boxed.

Supplementary Figure 2. Yeast surface display sort progressions of WT TACI (68-110) engineering mutagenesis by directed evolution. Dot plots are normalized to 100,000 events each. The R3 selection gate display cells were passaged to the next sort condition. **A.** First cycle of mutagenesis with alternating selections on decreasing concentrations of APRIL and BAFF to increase binding. **B.** Second cycle affinity maturation. The output DNA from cycle 1 affinity maturation was reformatted for in vitro screening and used as template for construction of a second error prone PCR library. **C.** Resultant mutagenized TACI sequences encoded a unique

variant TNFR domain, or 'vTD'. Mammalian expression constructs were generated by fusing the vTD sequences to a human IgG1-derived Fc coding region containing previously described mutations to reduce Fc receptor and complement interactions (41). Representative APRIL and BAFF inhibition curves from the TACI/Jurkat/NF-κB assay of 15 hits (black lines and TACI vTD H88 in green) obtained from the TACI engineering and yeast surface display. WT TACI 30-110-Fc is shown in purple, and the Fc control is in grey.

Supplementary Figure 3. Inhibition of BAFF multimers and BAFF/APRIL heterotrimers by povetacicept in the TACI/Jurkat/NF-κB assay relative to comparator molecules. **A.** BAFF 60-mer and **B-D.** heterotrimeric BAFF/APRIL and homotrimeric BAFF inhibition by povetacicept, TACI 30-110-Fc, telitacicept was sourced through Clinigen, belimumab was obtained from Myonex, and anti-APRIL mAb was based on the VIS649 mAb sequence. Curve fit with GraphPad Prism log(agonist) vs. Response. Constraints: Hillslope = -1, F = 50.

Supplementary Figure 4. Gating scheme for quantifying CD40L-stimulated human primary B cell subsets and plasma cells. **A.** Cells were gated away from debris in the FSC-A/SSC-A dot plot. Viable cells were confirmed as LiveDead blue negative and used with a FSC-H/FSC-A gate to exclude doublet cell populations. Class-switched (CSw) memory B cells were identified as IgM-IgD-CD27+CD38+. Plasma cells were identified as IgM-IgD- $CD38^{high}$ CD319+. **B.** Representative plots for CSw memory B cells and plasma cells from CD40L-stimulated human pan B cells cultured with 10 nM test articles or non-treated (APRIL and BAFF-only). FSC-A = forward scatter area; SSC-A = side scatter area; H = height; W = width.

Supplementary Figure 5. Povetacicept affects splenic B and T cell subsets more potently than WT TACI-Fc in KLH-immunized mice. Povetacicept, Fc control and WT TACI-Fc comparators were evaluated in a KLH mouse immunization model. C57BL/6NJ mice were challenged with KLH on Days 0 and 12 and povetacicept, Fc control, or WT TACI-Fc comparators (molar-matched to 10 mg/kg ALPN-303) were dosed IP on Days 4 and 11. **A.** On Day 20, total numbers of indicated splenic B cell subsets were enumerated by flow cytometry as described in Methods. **B.** Splenic T cells were also enumerated by flow cytometry. Individual mice are plotted, and the

mean ± SD shown as horizontal line and error bars, respectively. GC = germinal center; T1 = transitional-1 B cell; T2 = transitional-2 B cell; FOL = follicular; MZ = marginal zone.

Supplementary Figure 6. Gating scheme for quantifying B cell subsets and plasma cells in mouse spleens. Cells were gated away from debris in the FSC-A/SSC-A dot plot. This gate was analyzed by FSC-H/FSC-A and then SSC-H/SSC-W dot plots to gate cells along established diagonals that exclude doublet cell populations. The CD45+/LiveDead Aqua viability-negative cells were gated from the SSC-H/SSC-W singlet gate to identify live CD45+ cells. The live CD45+ cell gate was then analyzed by a B220/Gr1 dot plot. The B220+/Gr1- cells were then analyzed by a GL7/CD95 dot plot to identify GL7+/CD95+ GC B cells. B220+/Gr1- cells were also analyzed by a CD138/CD19 dot plot to identify CD19+ cells, which were subsequently analyzed by a CD23/CD19 dot plot. The CD23+/CD19+ cells were further analyzed by CD21/IgM expression to identify CD21+/IgM+ Follicular (FOL) B cells and $CD21^{br}/IgM^{br}$ T2 B cells. The CD23-/CD19+ cells were also analyzed by a CD21/IgM dot plot to identify CD21-/IgM^{br} transitional type-1 (T1) B cells and $CD21^{br}/IgM^{br}$ MZ B cells. The live CD45+ cell gate was also analyzed by a B220/CD19 dot plot to identify $B220^{+/lo}$/CD19+ B cells. The $B220^{lo}$/CD138+ plasma cells were gated from the $B220^{+/lo}$/CD19+ gate. FSC-A = forward scatter area; SSC-A = side scatter area; H = height; W = width.

Supplementary Figure 7. Gating scheme for quantifying CD4+ T_{FH} cells in mouse spleens. Cells were gated away from debris in the FSC-A/SSC-A dot plot. This gate was analyzed by FSC-H/FSC-A and then SSC-H/SSC-W dot plots to gate cells along established diagonals that exclude doublet cell populations. The CD45+/LiveDead Aqua viability-negative cells were gated from the SSC-H/SSC-W singlet gate to identify live CD45+ cells. The live CD45+ cell gate was then analyzed by a B220/CD3 dot plot. The CD3+ T cells were then analyzed by a CD4/CD8 dot plot. CD4+ T cells were analyzed by a PD1/CXCR5 dot plot to identify PD1+ CXCR5+ T_{FH} cells. T_{FH} = T follicular helper; FSC-A = forward scatter area; SSC-A = side scatter area; H = height; W = width.

Supplementary Figure 8. Povetacicept demonstrates enhanced immunosuppressive activity over telitacicept and anti-CD20 antibody in a mouse SRBC immunization model. Following

SRBC immunization on Day 0, female BALB/cJ mice were dosed twice (IP), on Days 1 and 6, with 10 mg/kg povetacicept or molar-matched Fc control or telitacicept (sourced through Clinigen); a depleting anti-mouse CD20 antibody was administered once on Day 1 (10 mg/kg). **A.** Anti-SRBC Ig serum levels were measured on Day 15. **B.** Percent plasma cells in bone marrow enumerated by flow cytometry, with data from individual mice plotted. Bone marrow was not collected from the naïve group. **C-D.** Total number of germinal center (GC) B cells/spleen or CD4+ T_{FH} cells/spleen, enumerated by flow cytometry, with individual mice plotted. Data are presented as mean ± SD.

Supplementary Materials and Methods

ELISA assays

Serum Anti-KLH Antibody ELISA

Serum samples were diluted and incubated in KLH-coated plates, washed, and detected with 1:2000 goat anti-mouse IgG1:horseradish peroxidase (HRP) or 1:5000 goat anti-mouse IgM:HRP (Jackson ImmunoResearch). Color development was with a 3,3′,5,5′-tetramethylbenzidine (TMB) Substrate Kit (SeraCare Life Sciences Inc) and analyzed on a plate reader (EMax® Plus Microplate Reader, Molecular Devices). Absorbance at 450 nM was used to measure anti-KLH IgM and IgG1 antibodies; there was no standard curve for the assay.

TACI Ig Detection ELISA

Anti-TACI (clone 165609, Invitrogen) was pre-coated in 96 well plate overnight. Study samples were minimally diluted 1:100 to target the assay calibration range and incubated along with assay calibrators and controls matched to test article (povetacicept and WT TACI 13-118-Fc). Bound test article was probed by incubation with HRP-conjugated Fc-specific mouse anti-human IgG (Jackson ImmunoResearch) followed by addition of the HRP substrate 3,3′,5,5′-TMB. The absorbance signal was visualized on an iD3 microplate reader (Molecular Devices). Test article concentrations in the study samples and assay controls were calculated from the test article-matched calibration curve.

Flow Cytometry Gating

Mouse B and T cell subsets were defined by gating as follows: Germinal Center (GC) B cells (CD45+, B220+, CD19+, GL7+, CD95+), Plasma Cells (CD45+, B220-, CD19+, $CD138^{high}$ or $TACI^{high}$, $CD138^{high}$ live single cells), Plasmablasts ($TACI^{high}$, $CD138^{high}$, B220+, CD19+ live single cells), Long-Lived Plasma Cells ($TACI^{high}$, $CD138^{high}$, B220-, CD19- live cells), Marginal Zone (MZ) B Cells (CD45+, B220+, CD19+, CD23-, $CD21^{high}$, IgM^{high}), Transitional Type 1 (T1) B Cells (CD45+, B220+, CD19+, CD23-, CD21-, IgM+), Transitional Type 2 (T2) B Cells (CD45+, B220+, CD19+, CD23+, $CD21^{high}$, IgM^{high}), Follicular B Cells (CD45+, B220+, CD19+, CD23+, CD21+, IgM+), CD8+ T Cells (CD45+, CD3+, CD8+), CD4+ T Cells (CD4+,

CD3+, CD4+), and CD4 T Follicular Helper (T_{FH}) Cells (CD45+, CD3+, CD4+, PD1+, CD185+).

Povetacicept: An Enhanced Dual APRIL/BAFF Antagonist that Potently Modulates B Lymphocytes and Pathogenic Autoantibodies

APRIL and BAFF are key drivers of pathogenic autoantibody production

Povetacicept treatment reduces autoantibodies and end-organ disease in lupus models

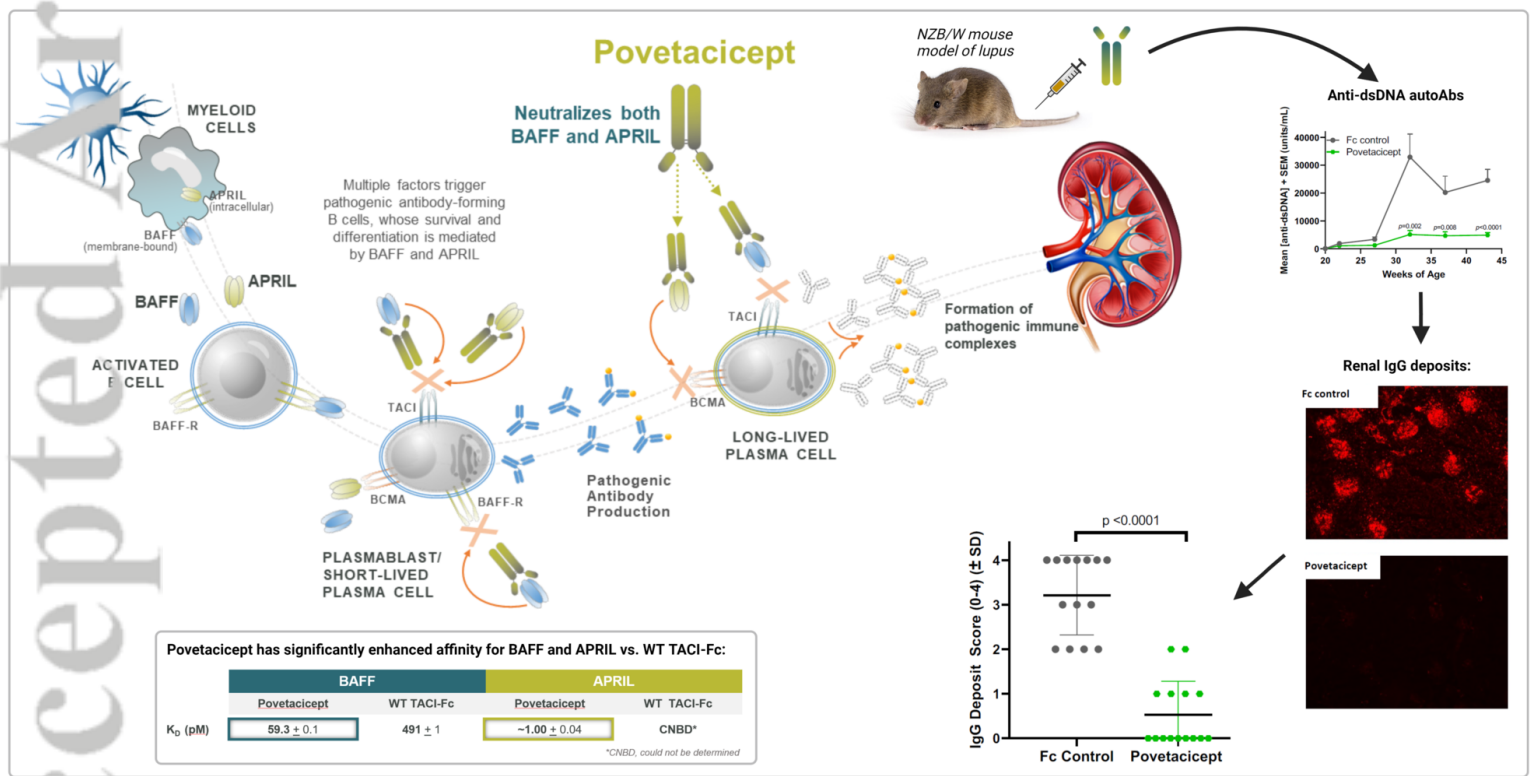

Povetacicept has significantly enhanced affinity for BAFF and APRIL vs. WT TACI-Fc:

	BAFF		APRIL	
	Povetacicept	WT TACI-Fc	Povetacicept	WT TACI-Fc
K_D (pM)	59.3 ± 0.1	491 ± 1	~1.00 ± 0.04	CNBD*

*CNBD, could not be determined

Evans LS, Lewis KE, DeMonte, et al. Povetacicept, an enhanced dual APRIL/BAFF antagonist that modulates B Lymphocytes and pathogenic autoantibodies for the treatment of lupus and other B cell–related autoimmune diseases. Arthritis Rheumatol 2023.

Arthritis & Rheumatology ACR American College of Rheumatology

ART_42462_Dillon_GraphicalAbstract_ar-22-1460 REVISED.png

A

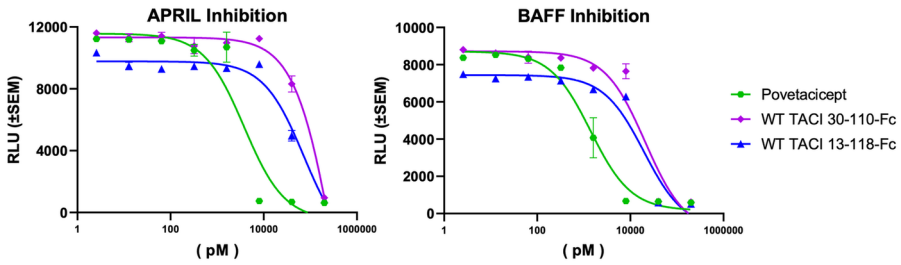

B

Test Article	Sample	$k_{a\ app}$ 1x10^{9} ($M^{-1}s^{-1}$)	$k_{d\ app}$ 1x10^{-3} (s^{-1})	R_{max} (RU)	$K_{D\ app}$ (pM)
Povetacicept	APRIL	7.0 ± 7	7.0 ± 6	55.5 ± 0.1	1.00 ± 0.04
Telitacicept	APRIL	CNBD*	CNBD	CNBD	CNBD

Test Article	Sample	k_a 1x10^{5} ($M^{-1}s^{-1}$)	k_d 1x10^{-5} (s^{-1})	R_{max} (RU)	K_D (pM)
Povetacicept	BAFF	6.19 ± 0.01	3.67 ± 0.02	52.8 ± 0.3	59.3 ± 0.1
Telitacicept	BAFF	1.75 ± 0.01	8.63 ± 0.02	47.6 ± 0.4	491 ± 1

**CNBD – could not be determined*

C

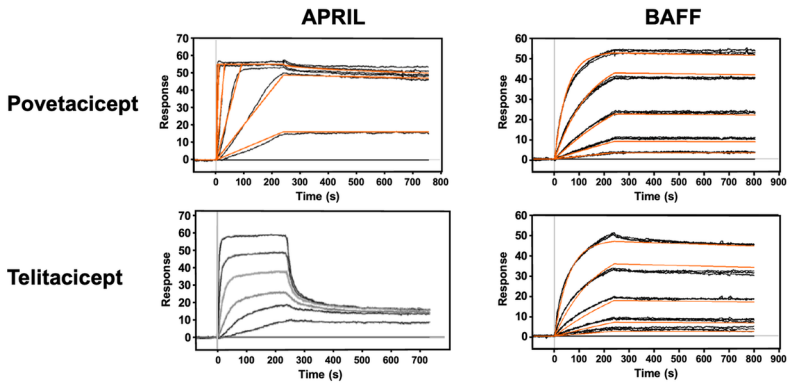

ART_42462_Figure 1.tif

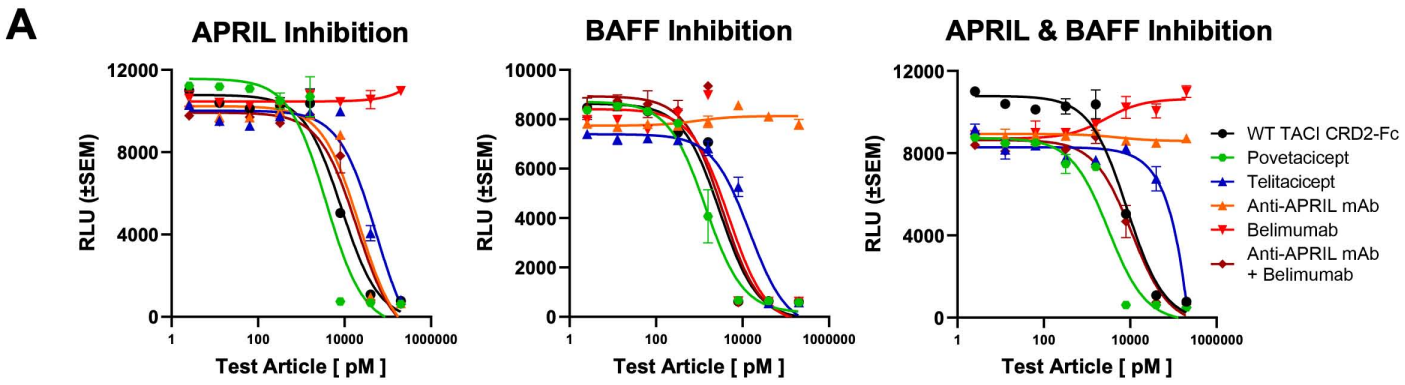

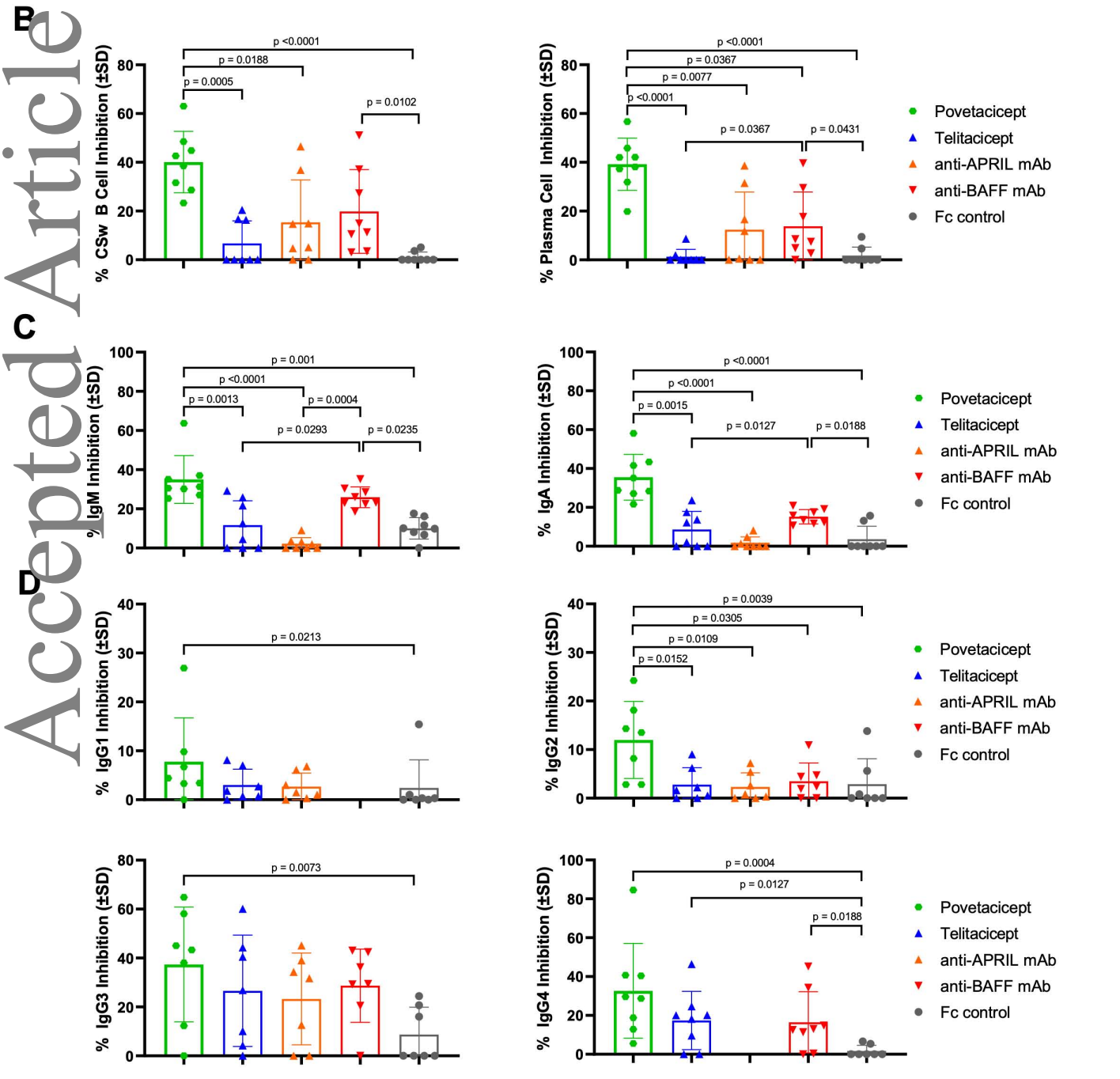

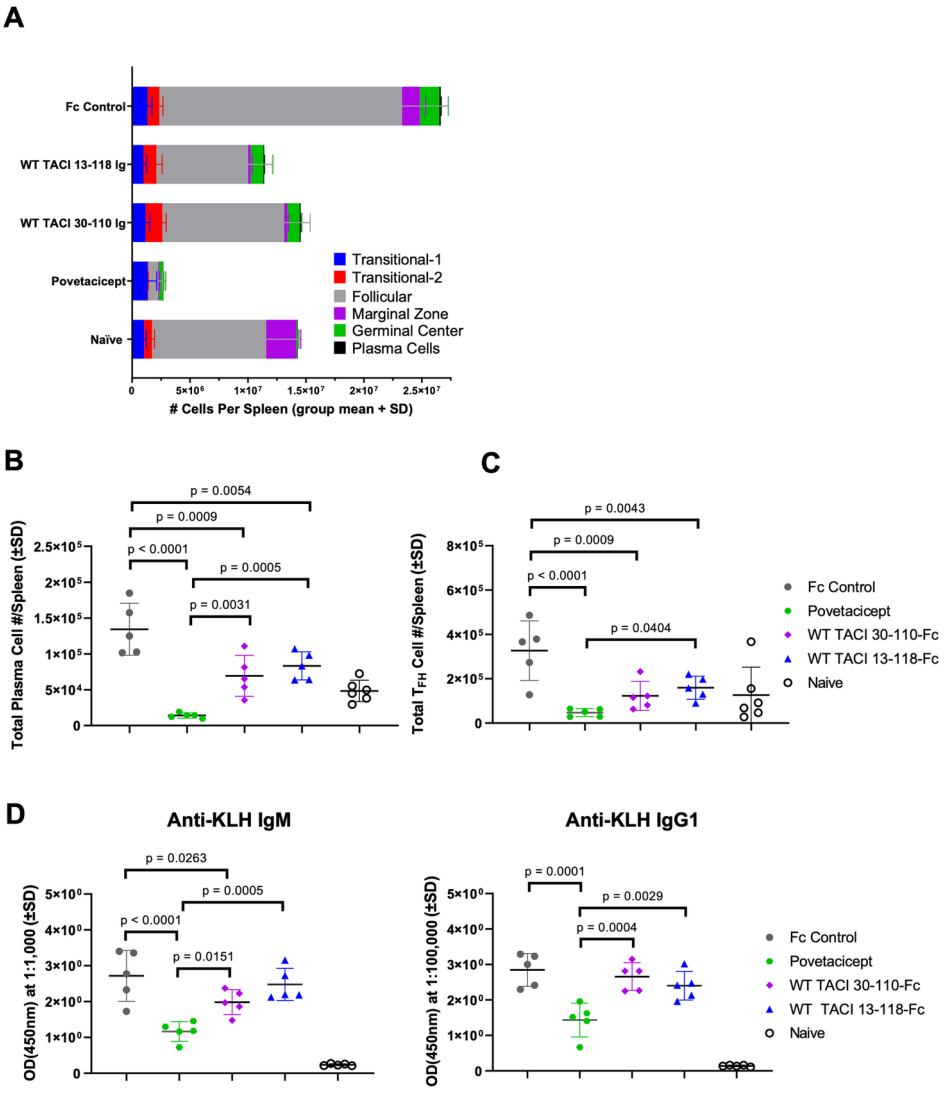

ART_42462_Figure 3.tif

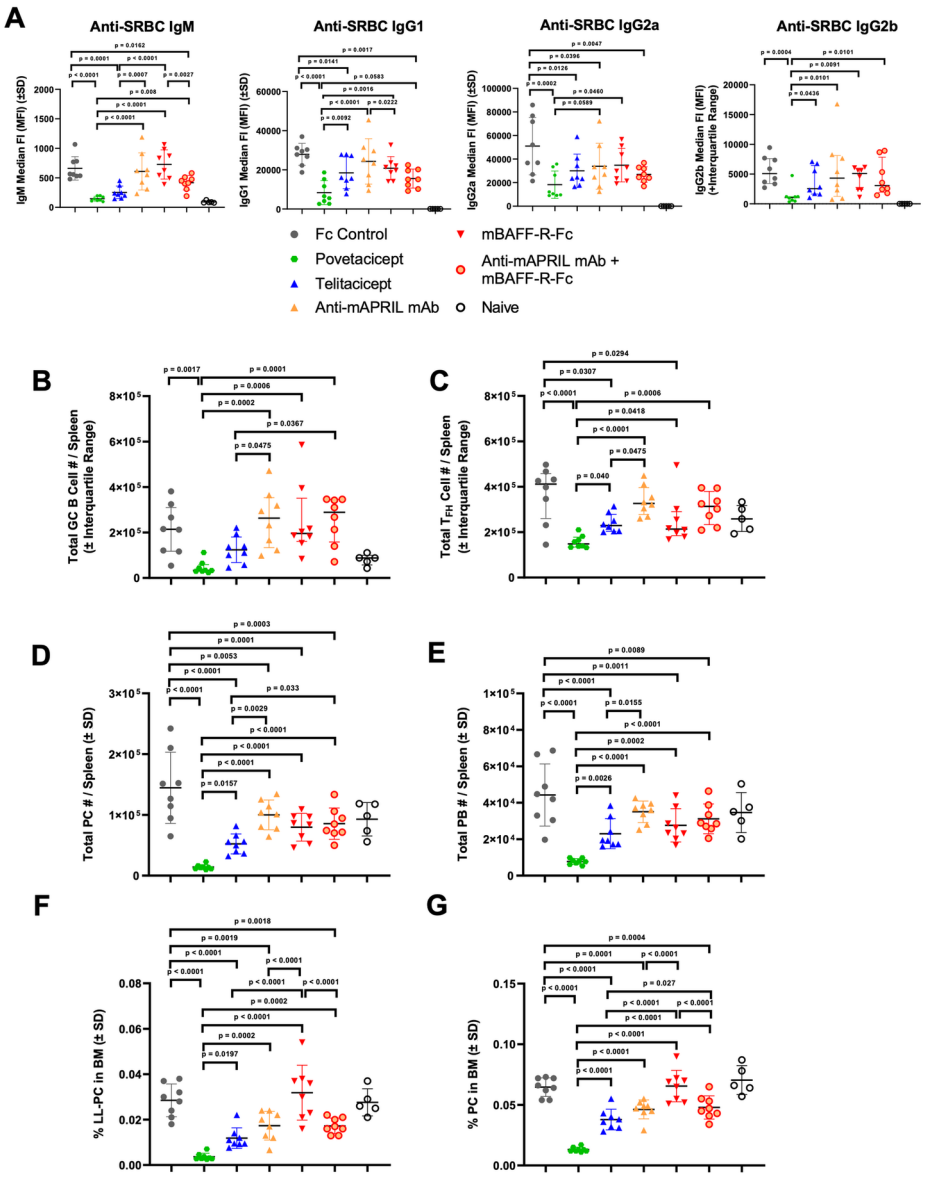

ART_42462_Figure 4.tif

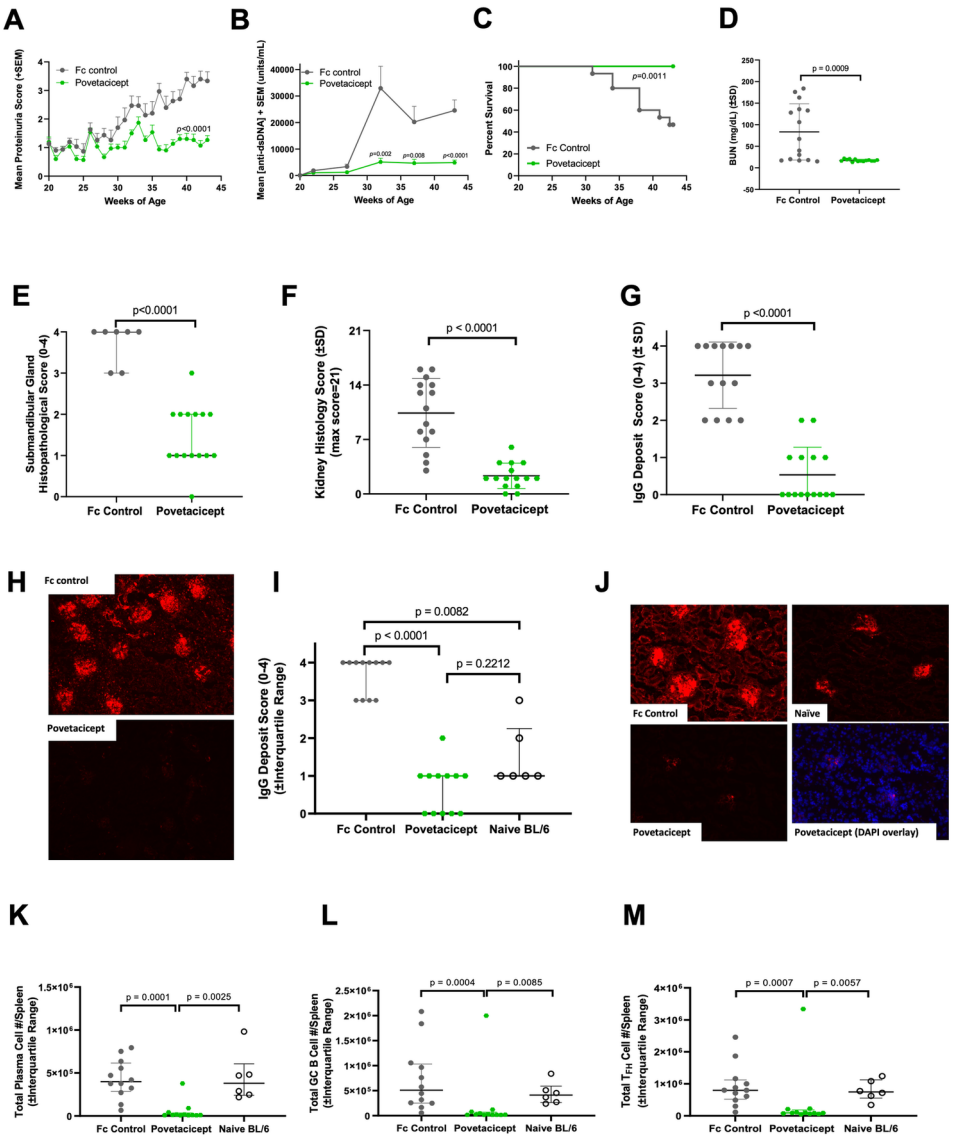

ART_42462_Figure 5.tif

A

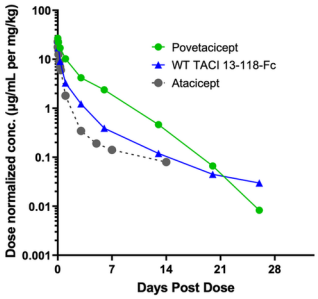

Noncompartmental PK Parameters

	C_{max}/Dose (µg/mL per mg/kg)	AUC/Dose (µg*hr/mL per mg/kg)
Povetacicept	27	1167
WT TACI 13-118-Fc	25	397
Atacicept	23	215*

*Note: Atacicept value is reported as $AUC_{0\text{-}inf}$, not $AUC_{0\text{-}t}$

B

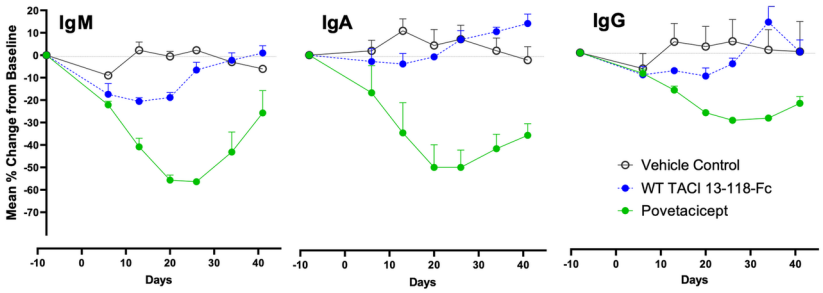

ART_42462_Figure 6.tif